

COMBUSTION IN SUPERSONIC FLOWS

UKCTRF

September 13th 2022, Newcastle University



P. Domingo, G. Ribert
J. Ruan, E. Yhuel

CORIA-CNRS UMR6614
Rouen, FRANCE



COMBUSTION IN SUPERSONIC FLOWS

- Understanding and predicting combustion in supersonic flows = challenge,
- Few experiments on which to rely with limited diagnostics,
- Numerical simulations feasible but lack of validation, dissipation is an issue, few specific models (RANS or LES) for highly compressible reactive flows.

Two main applications: propulsion and security



As an illustration:

- 1- Large Eddy Simulation of a cavity-based scramjet combustor
- 2- Direct numerical simulation of a flame/shock interaction in a shock tube

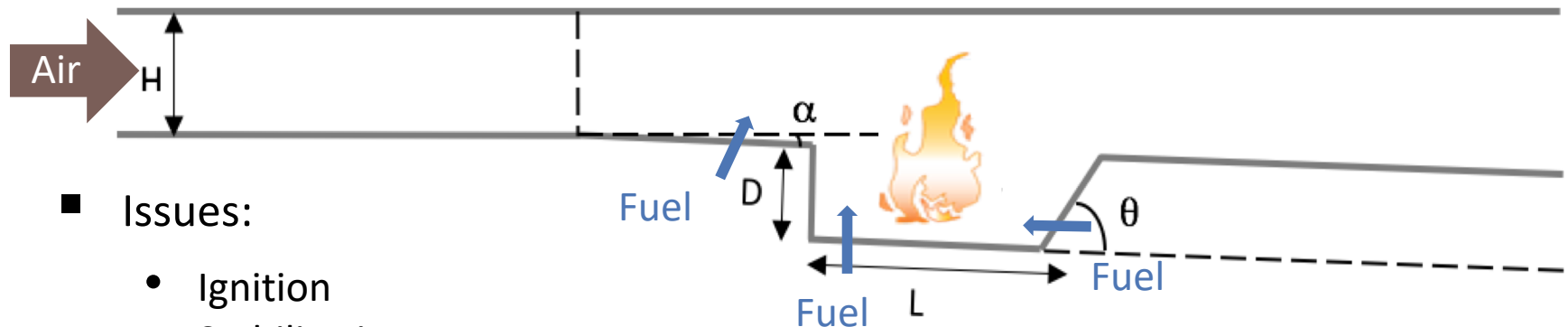
COMBUSTION IN SUPERSONIC FLOWS: the scramjet

■ What is a SCRAMJET?

- Engine flying at Mach 5-15
- No moving parts (compressor/turbine)
- The incoming air flow stays at supersonic speeds but reduced through compressive shocks
- **Short time left for mixing and combustion**
- Cavity, a promising flame holding device
- Fuel injection may be performed upstream or inside the cavity



NASA X-43A, Mach 10



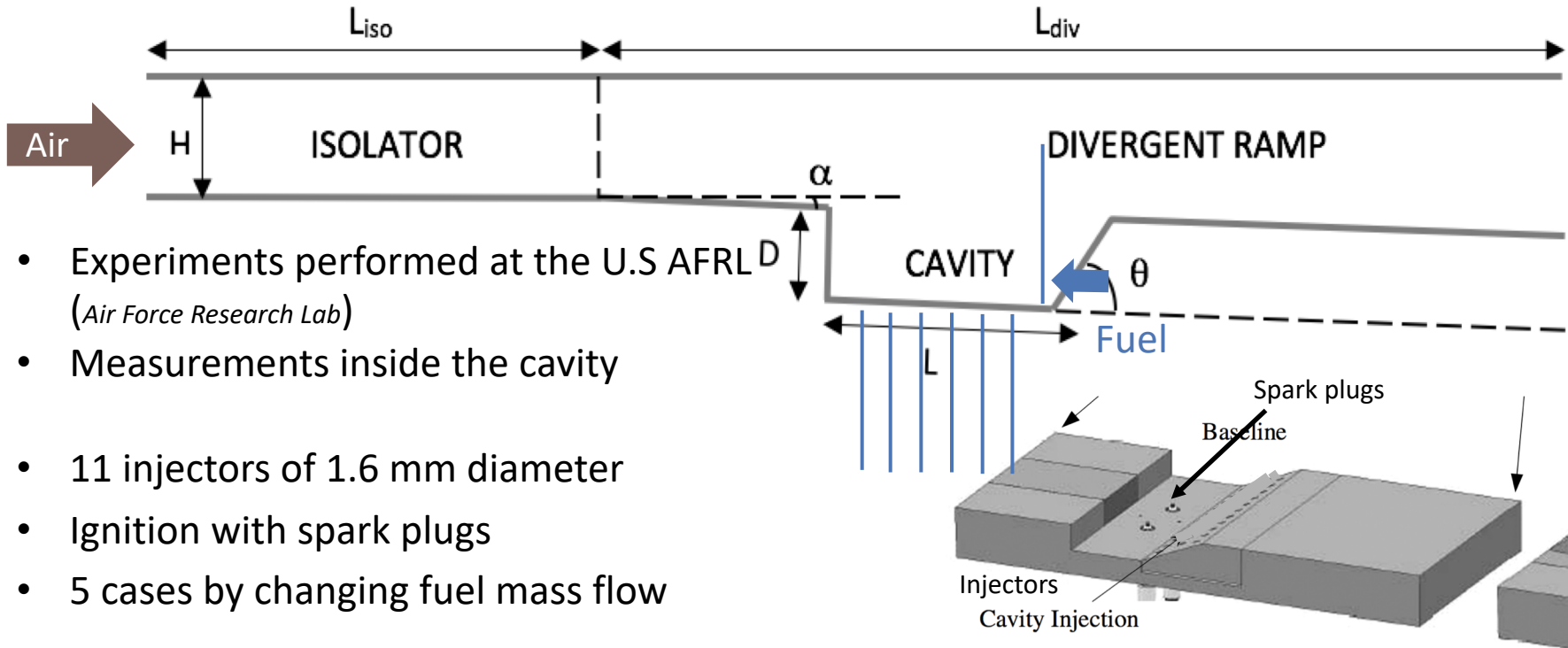
■ Issues:

- Ignition
- Stabilization
- Impact of wall heat transfer

LES to investigate these issues

Experimental configuration

Dimensions : 390 x 72.7 x 152.4 mm³



- Experiments performed at the U.S AFRL D (Air Force Research Lab)
- Measurements inside the cavity
- 11 injectors of 1.6 mm diameter
- Ignition with spark plugs
- 5 cases by changing fuel mass flow

Case	1	2	3	4	5
T_o , K	589	589	589	589	589
P_o , kPa	483	483	483	483	483
Mach	2	2	2	2	2
U_∞	727	727	727	727	727
Fuel, SLPM	0	56	99	39 → 36	110

Fuel	Ethylene
L/D	4
θ	22.5°
Injection	Ramp injection

Numerical solver

<https://www.coria-cfd.fr/index.php/SiTCom-B>

Main features of SiTComB

Fully compressible explicit structured code-Finite Volume code

Immersed Boundary Method (IBM) for complex geometry

4th order centered scheme for diffusive terms

4th order centered skew-symmetry-like scheme for convective terms

Ducros et al., JCP, Vol 152, 1999

4th order Runge-Kutta method for time integration

Jiang et al., JCP, Vol 126, 1996; Gottlieb et al., MC, Vol 67, 1998

Full multi-species formulation

Complex chemistry

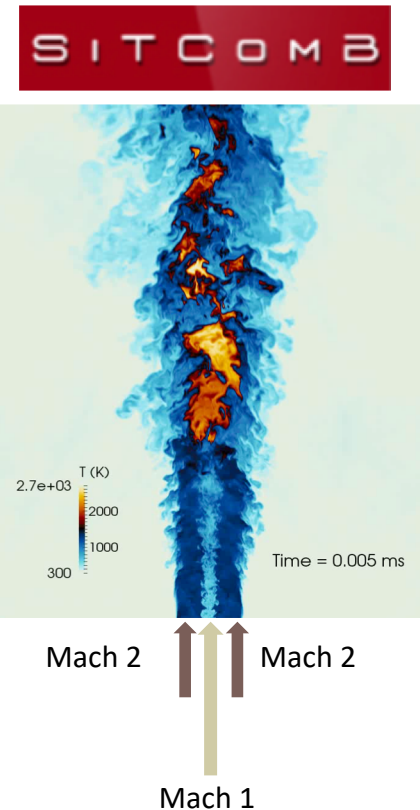
Artificial dissipation

Swanson et al., JCP, Vol 101, 1992; Tatsumi et al., AIAA Journal, Vol 33, 1995;
Swanson et al., JCP, Vol 147, 1998

3D-NSCBC boundary treatment

Lodato et al., JCP, Vol 227, 2008

- Validated for supersonic combustion by Bouheraoua et al. [1] in the configuration of the burner of Cheng et al. [2]
- Validated for supersonic combustion and discontinuities capture by Guven et al. [3]

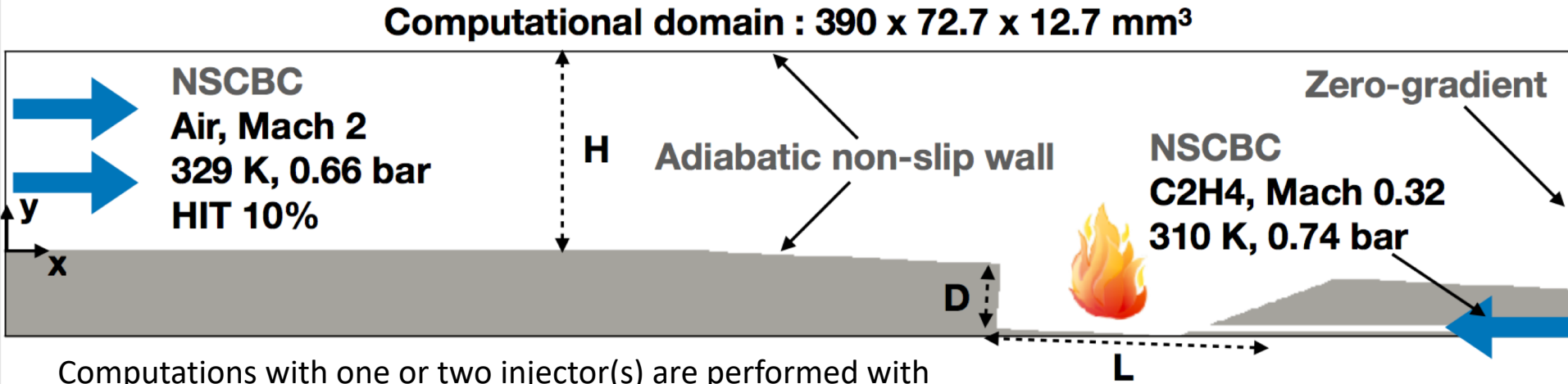


[1] Bouheraoua et al., *Combust. Flame*, Vol 179, 2017

[2] Cheng et al., *Combust. Flame*, Vol 99, 1994

[3] Guven et al., *J. Propul. Power*, Vol 34, 2018

Numerical set-up configuration



Computations with one or two injector(s) are performed with periodic conditions on both sides.

MESH	Δx (μm)	Δy (μm)	Δz (μm)	CELLS ($\times 10^6$)
MESH 1	100	80 - 150	100 - 150	300
MESH 2	200	150 - 200	160 - 300	45

Unsolved fluxes modeling : Dynamic Smagorinsky subgrid-scale model

Germano et al., *Phys. Fluids* 3(7), 1991; Moin et al., *Phys. Fluids* 7(3), 1991; Lilly, *Phys. Fluids* 4(3), 1992

Laminar model : No-model

$$\tilde{\omega}_k(\rho, \underline{Y}, T) \approx \dot{\omega}_k(\bar{\rho}, \tilde{\underline{Y}}, \tilde{T})$$

Numerical tests

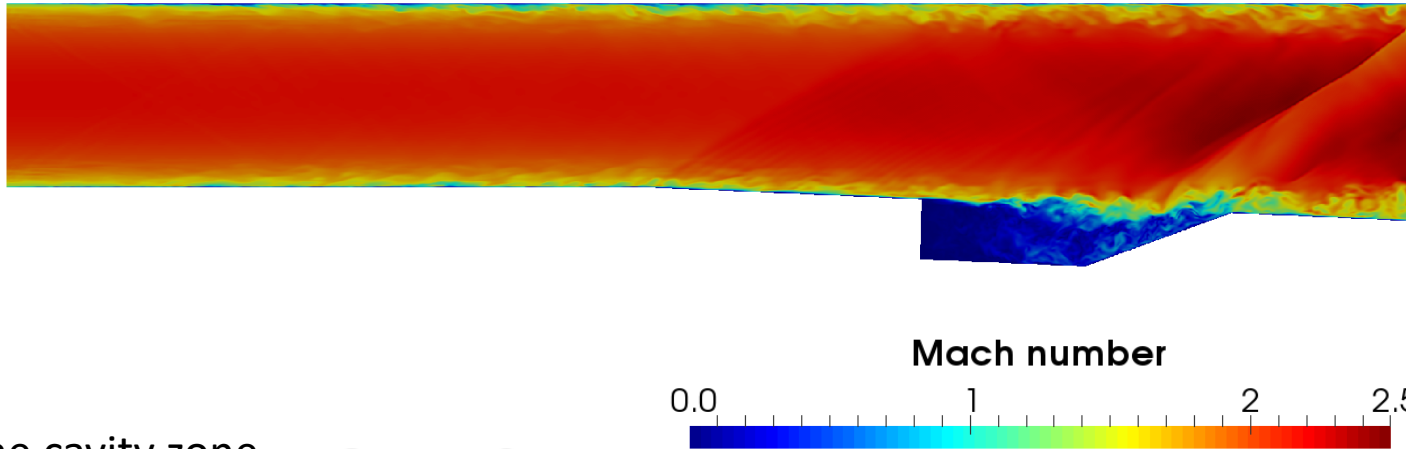
- Assess the possibility of the LES to reproduce the available experimental results for four of the experimental cases (no fuel injection, Medium High Fuel Loading (MHF), Medium Fuel Loading, Lean fuel loading (LF))
- Available experimental results: velocity fields, wall-pressure, identification of stable and unstable cases, equivalent ethylene concentration
- Investigate the impact of the numerical set-up:
 - Mesh resolution
 - Wall thermal condition (adiabatic or isothermal)
 - Number of injectors included in the simulation (1, 2 or 11 including the lateral walls)
- Analyze the flame stabilization mechanism

The resulting data-base comprehends around 10 cases, the cost of a simulation with well converged statistics ranges from 100 000 hours up to 4 millions (non reactive 1 injector on coarse mesh compared to reactive 1 injector on fine mesh).

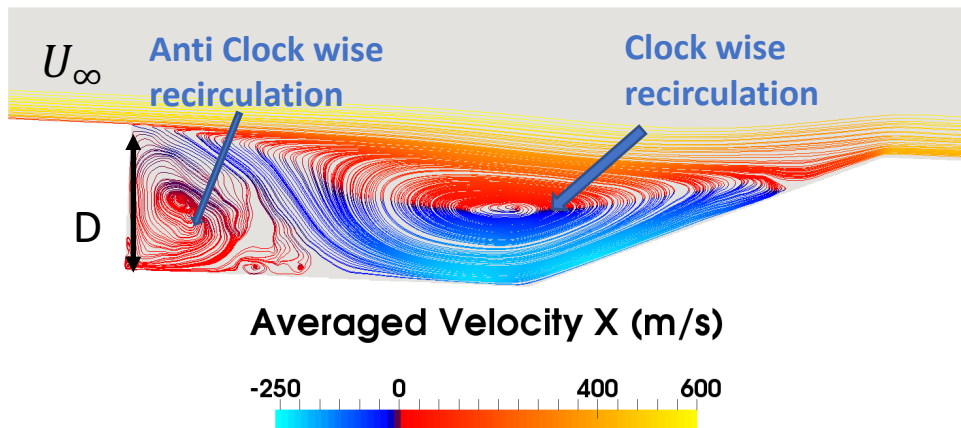
Many thanks to GENCI and CRIANN for providing cpu time!

Non reacting flow

2D-cut of instantaneous Mach number field for the coarse mesh



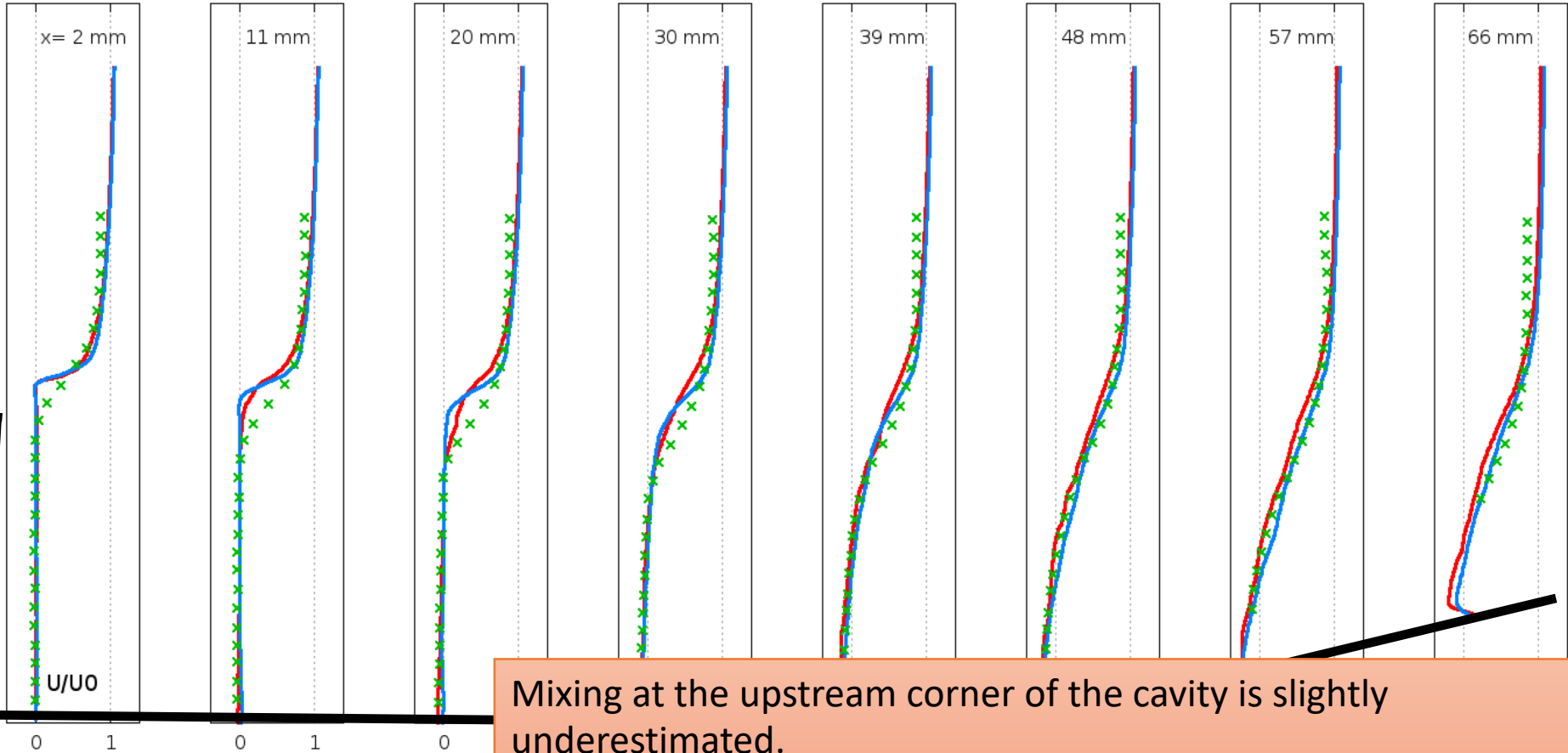
Zoom on the cavity zone



- Whole cavity at subsonic speeds
- Clockwise recirculation (Mach ~ 0.5): drives the dynamics of the flow entering the cavity and promotes mixing of fresh air and fuel.
- Anti-clockwise recirculation (Mach < 0.1): 'dead zone'.

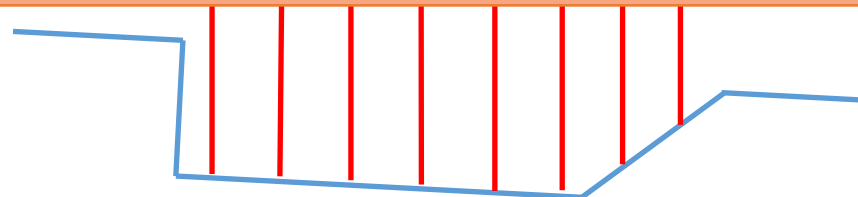
Non reacting flow

Averaged streamwise velocity



Mixing at the upstream corner of the cavity is slightly underestimated.
Good agreement at all other locations.

- MESH 1 (fine)
- MESH 2 (coarse)
- × Experiment

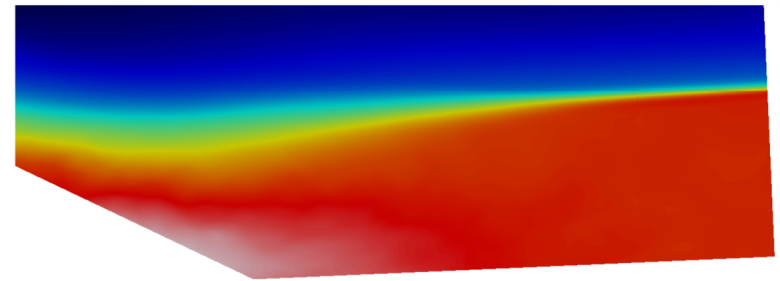
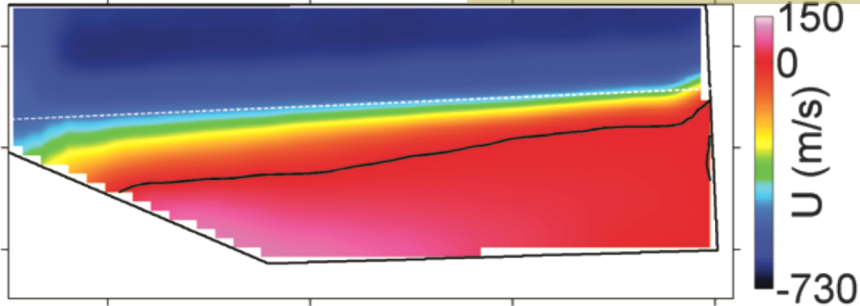


Non reacting flow (coarse mesh)

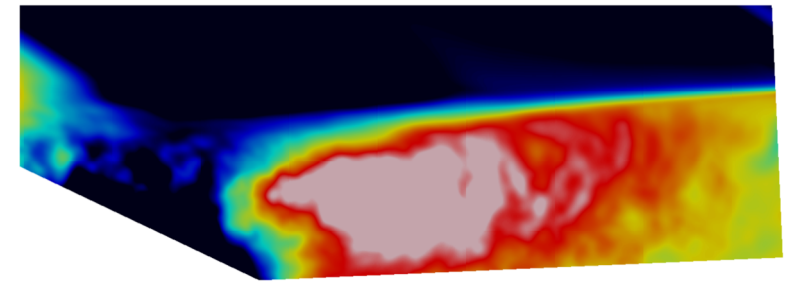
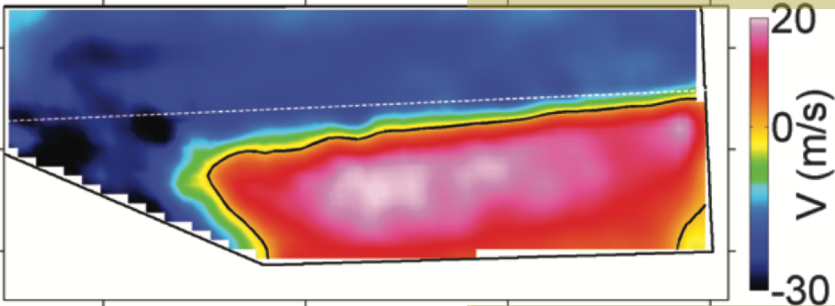
Experiment

Simulation

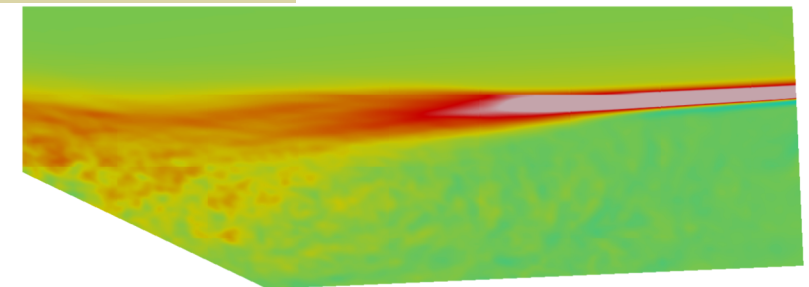
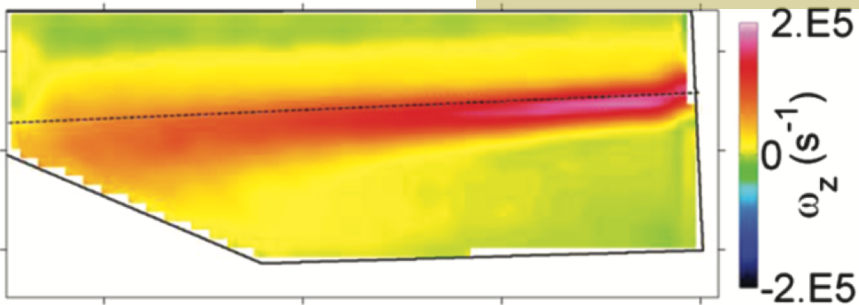
Averaged streamwise velocity



Averaged tranverse velocity



Average vorticity

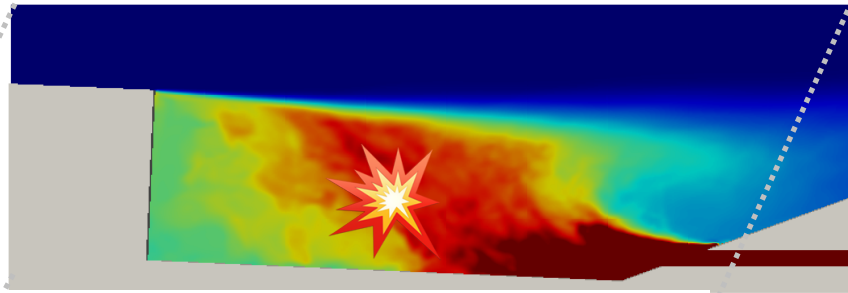


X



Fuel injection and ignition

Injector centerplane



Averaged Fuel air equivalence ratio snapshots at the center plane of the injector and the center plane between two injectors without combustion

$$\Phi = \frac{Y_F}{Y_O} \left(\frac{Y_O}{Y_F} \right)_{st}$$

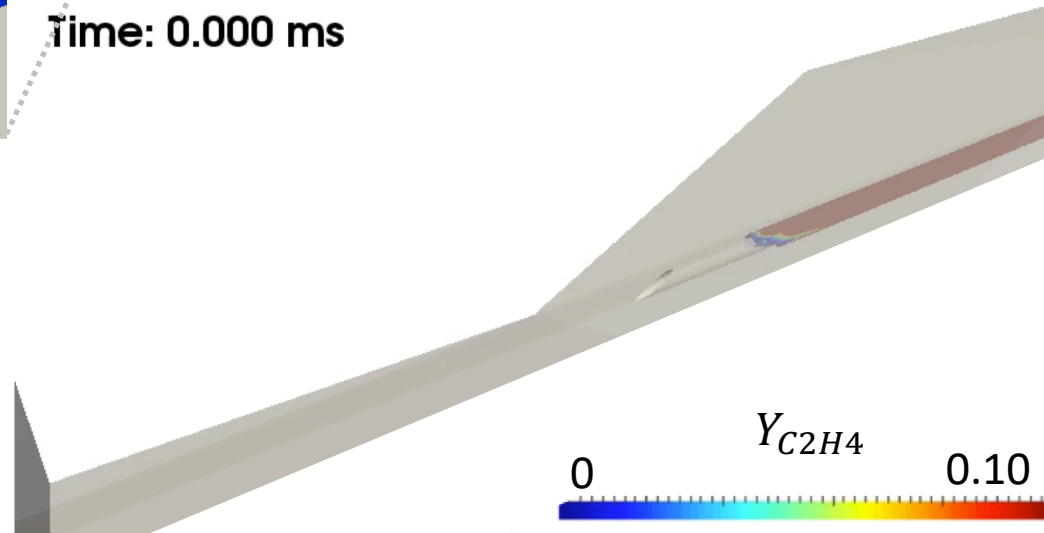
Time: 0.000 ms

Fuel-air equivalence ratio

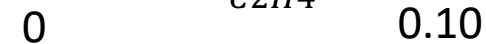


Centerplane between 2 injectors

Ignition source kept for 1 ms



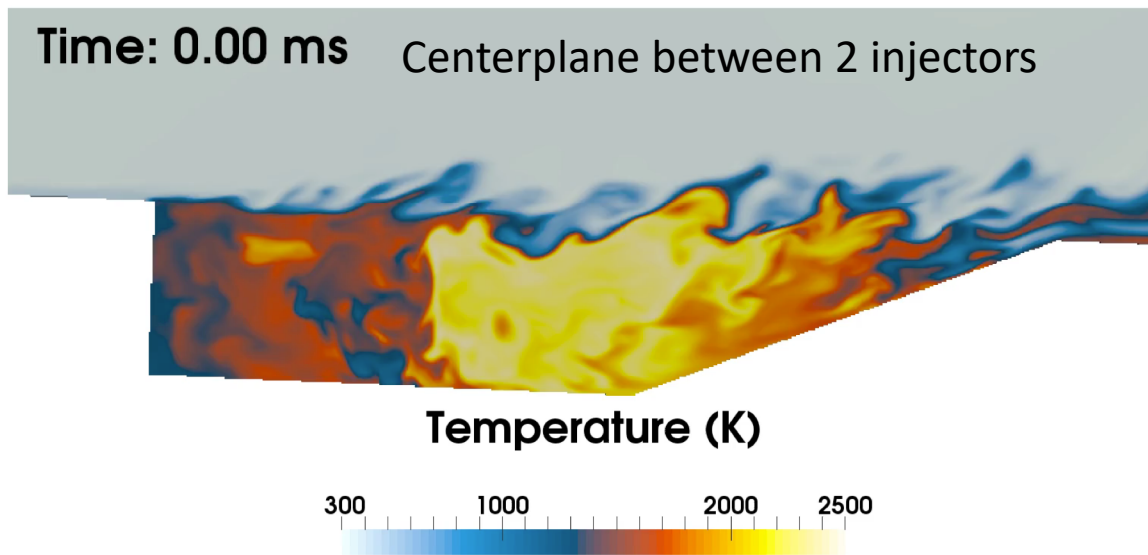
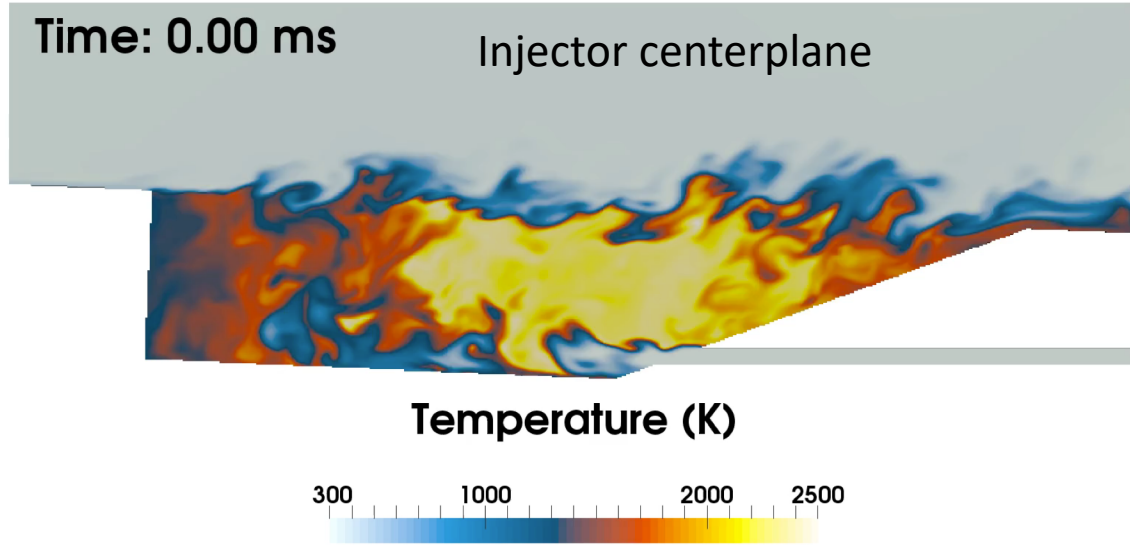
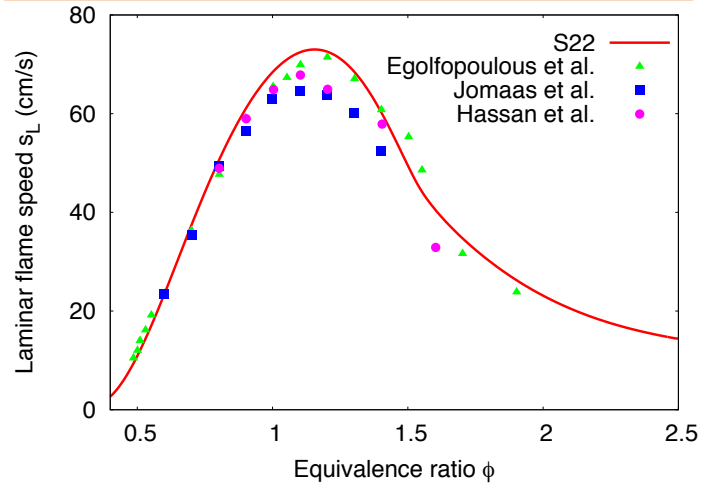
$Y_{C_2H_4}$



Reacting flow

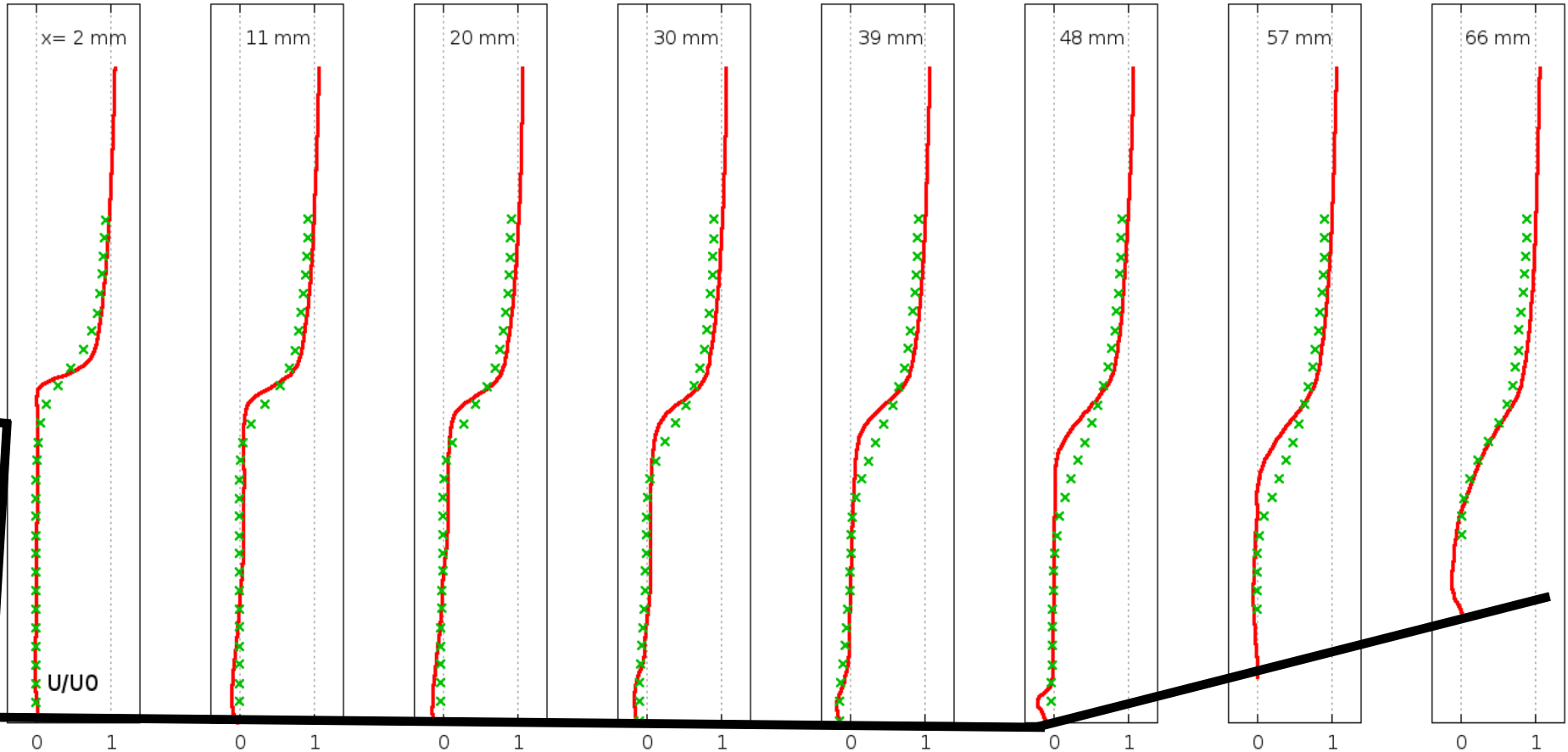
22 species / 206 reactions kinetic scheme

Luo et al., Combust. Flame, Vol 159, 2012

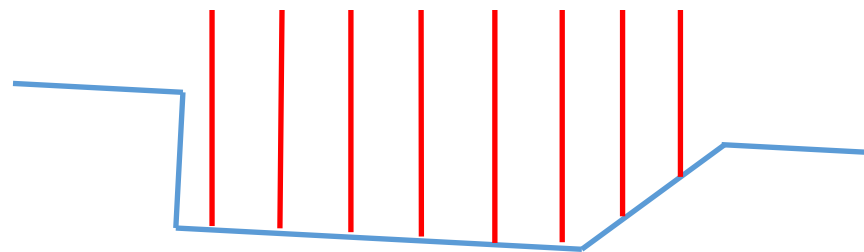


Reacting flow (fine mesh, MHF)

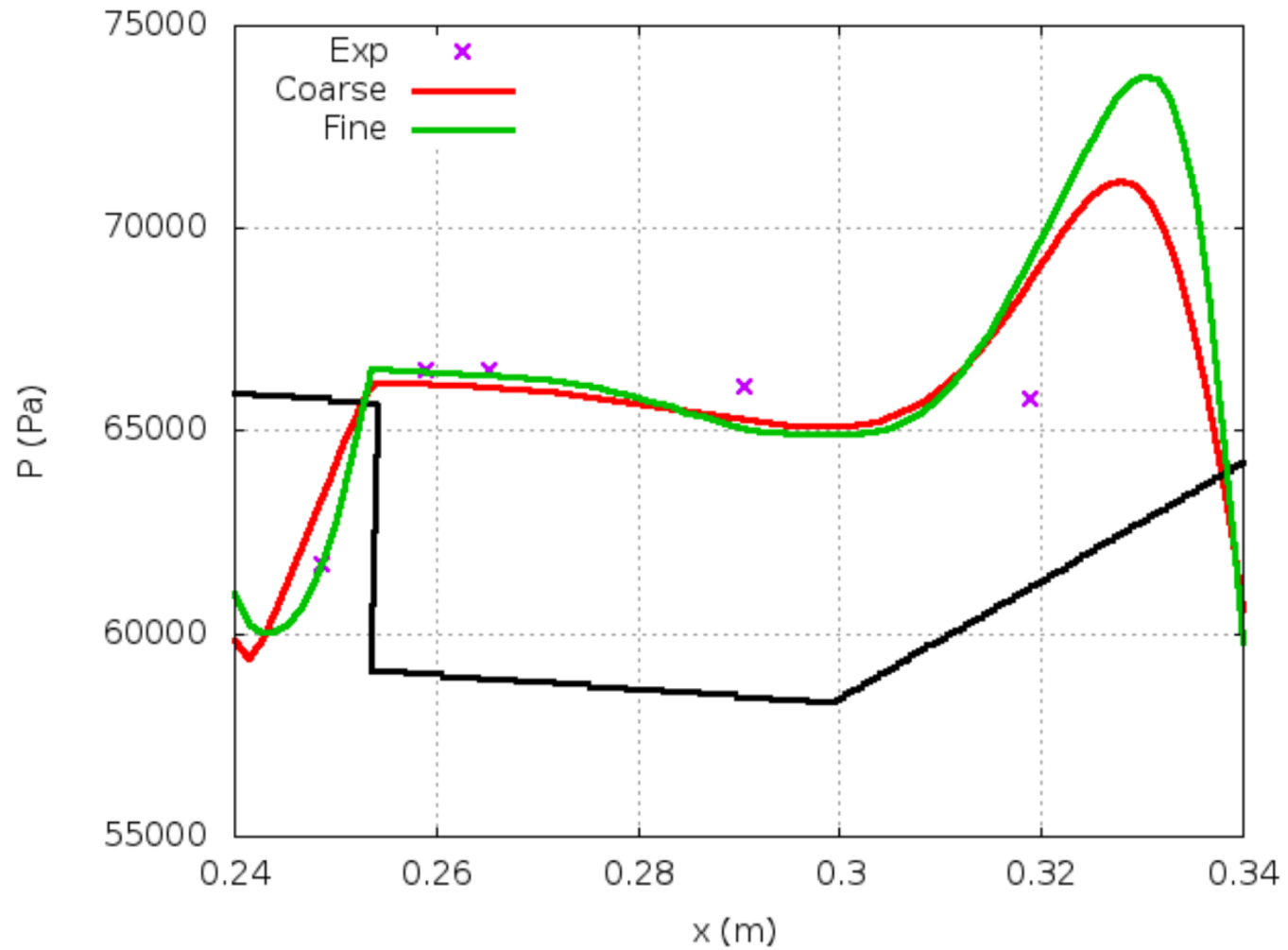
Averaged streamwise velocity



— Simulation
× Experiment



Wall pressure (MHF)



Flame stability function of ethylene mass flow rate

Case	1	2	3	4	5
T_o , K	589	589	589	589	589
P_o , kPa	483	483	483	483	483
Mach	2	2	2	2	2
U_∞	727	727	727	727	727
Fuel, SLPM	0	56	99	39 → 36	110

Experiment

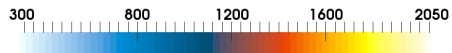
Cases 2 and 3 : stable combustion

Case 4 : extinction

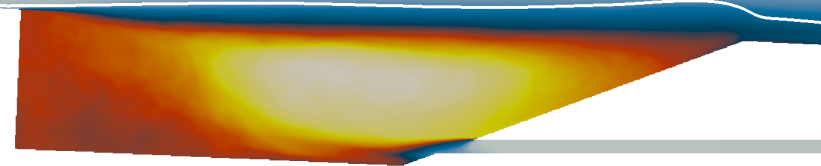
Case 2 (MF)



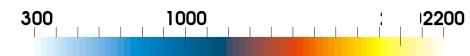
Averaged Temperature (K)



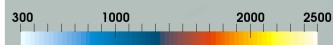
Case 3 (MHF)



Averaged Temperature (K)



Temperature (K)



Case 4 (LF)

Time: 4 ms



Discussion of the laminar assumption

Hypothesis of laminar model

$$\tilde{\omega}_k(\rho, \underline{Y}, T) \approx \dot{\omega}_k(\bar{\rho}, \underline{\tilde{Y}}, \tilde{T})$$

Subgrid Damköhler number criterion :

$$Da_{sgs} = \frac{\tau_{sgs}}{\tau_c}$$

Krol et al., J. Geophys. Research, Vol 105, 2000

Duwig et al., Combust. Theory and Modelling, Vol 15, 2011

- For $Da_{sgs} > 1$, segregations at SGS of the reacting species have to be accounted for.
- For $Da_{sgs} \ll 1$, all the relevant scales of the reacting species are adequately solved by means of the LES.

Subgrid Damköhler number

$$Da_{sgs} = \frac{\tau_{sgs}}{\tau_c}$$

$$(1) \quad \tau_{sgs} = \frac{C_s^2 \Delta^2}{\nu_t}$$

$$(2) \quad \tau_{sgs} = \frac{\Delta}{u_\Delta}$$

$$(3) \quad \tau_{sgs} = 0.86 \frac{\Delta^{3/4} \nu^{1/4}}{u_\Delta^{5/4}}$$

$$\tau_c = \min(\tau_{c,k})$$

$$\tau_{c,k} = \frac{\rho Y_k}{\dot{\omega}_k}$$

$$k = CO, CO_2, H_2O$$

$$u_\Delta = \sqrt{\frac{2}{3} \frac{\nu_t}{c_k \Delta}} \quad \text{with } c_k = 0.07$$

(1) Bouheraoua et al., Combust. Flame 179 (199-218)

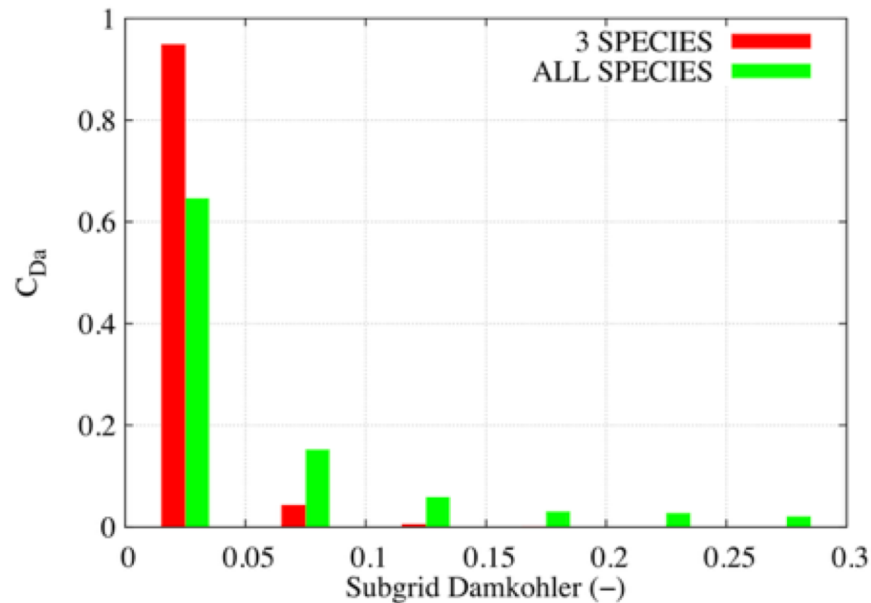
(2) Duwig et al., Combust. Theory Model 15(4)

(3) Moule et al., Combust. Flame 161(2647-2668)

Is the SGS Damköhler small enough?

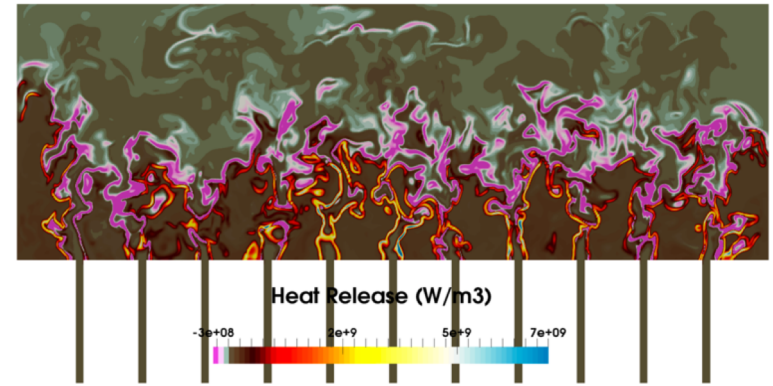
Only cells with relevant heat release rate are included in statistics

$$\dot{\omega}_E > 0.01\dot{\omega}_{E,max}$$



Cell ratio in each interval of subgrid Damköhler number.

$k = \text{all } 22 \text{ species}$



- Largely smaller than 1, whatever the definition of the chemical time retained (based on major species or all species).
- Determining the source terms from the transported value is OK!

$$\tau_{sgs} = \frac{C_s^2 \Delta^2}{\nu_t}$$

$$\tau_c = \min(\tau_{c,k})$$

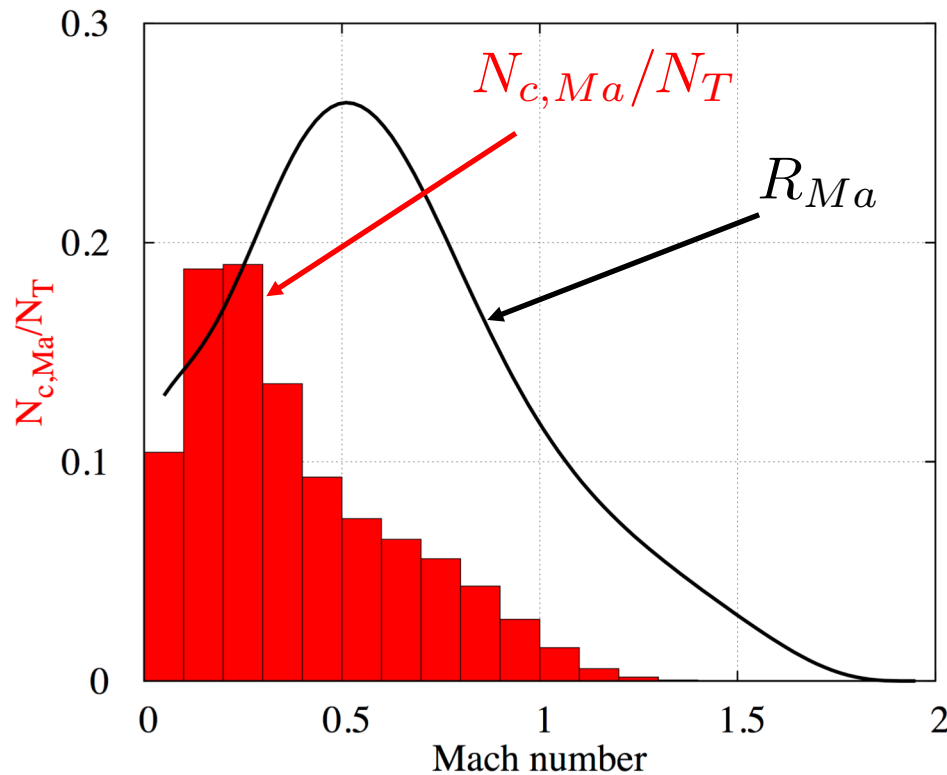
$$\tau_{c,k} = \frac{\rho Y_k}{\dot{\omega}_k}$$

Subsonic or supersonic combustion?

Only cells with relevant HRR included in the statistics:

$$\dot{\omega}_E > 0.01\dot{\omega}_{E,max}$$

Number of cells in each interval of Mach number



Conditional mean of heat release on Mach number

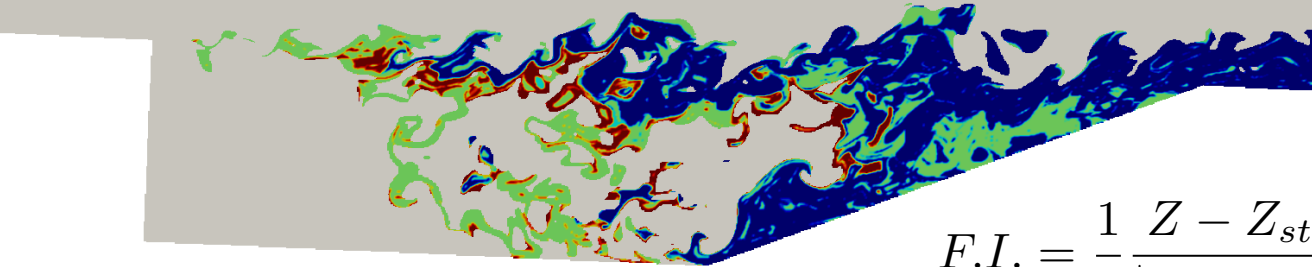
$$R_{Ma} = \frac{\langle \dot{\omega}_E | Ma \rangle}{\langle \dot{\omega}_E \rangle}$$

R_{Ma}

- Combustion occurs mostly at subsonic speeds: over 70% for $M < 0.6$ and over 95% for $M < 1$
- Maximum chemical activity at Mach 0.5

What kind of combustion regime? Case MHF

$$\dot{\omega}_E > 0.01\dot{\omega}_{E,max}$$



-1 0 1 **Flame Index (-)**

$$F.I. = \frac{1}{2} \frac{Z - Z_{st}}{|Z - Z_{st}|} \times \left(1 + \frac{\nabla Y_F \cdot \nabla Y_{O_2}}{|\nabla Y_F \cdot \nabla Y_{O_2}|} \right)$$

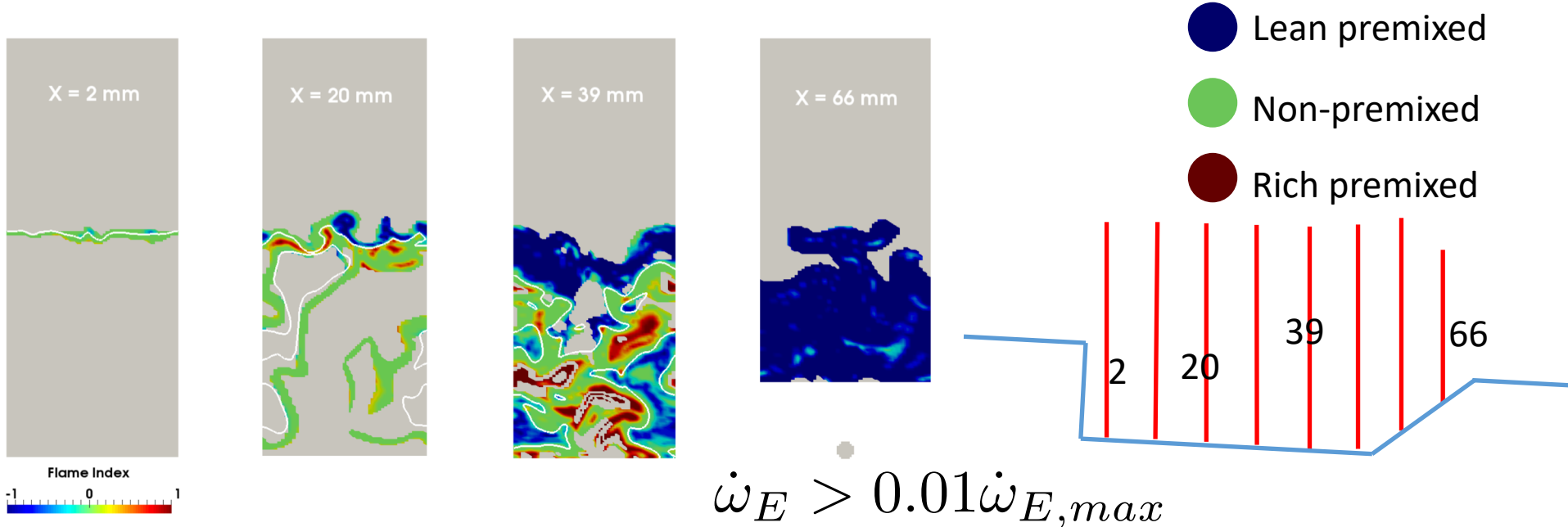
- Lean premixed
- Non-premixed
- Rich premixed

Z : mixture fraction from Bilger et al.'s expression

Y_F : mass fraction of ethylene and of its pyrolysis products

- Front of Cavity: mainly controlled by non-premixed combustion
- Middle of Cavity: the three regimes of combustion can be encountered
- Rear of Cavity: lean premixed combustion predominates (75%) followed by the non-premixed one

What kind of combustion regime? Case MF

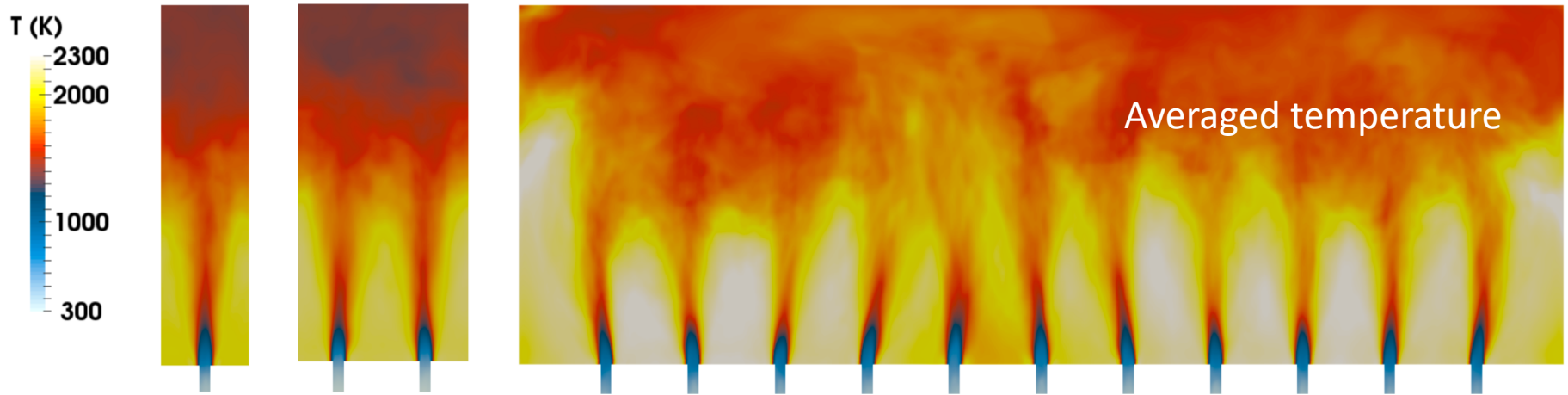


- Front of Cavity: mainly controlled by non-premixed combustion
- Middle of Cavity: the three regimes of combustion can be encountered **but with more non-premixed combustion than for MHF**
- Rear of Cavity: lean combustion predominates (75%) followed by the non-premixed one

Distribution of combustion regime varies with ethylene mass flow rate.

Impact of the number of injectors

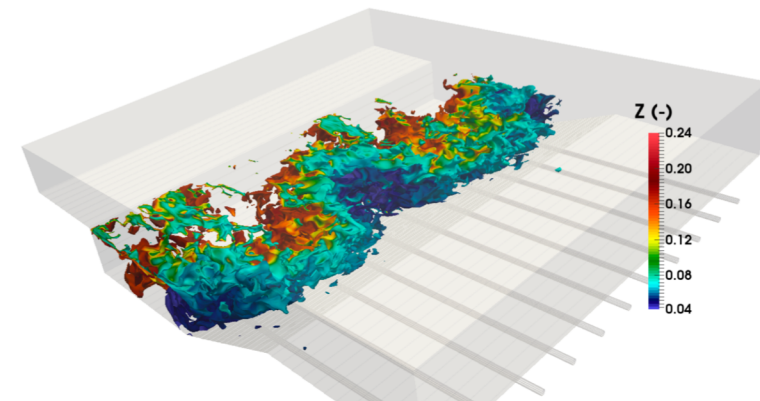
Simulations have been done with 1, 2 and 11 injectors:



Case	Cavity width (mm)	Injector center coordinate (mm)	Side boundary conditions
RCA1	12.7	$z = -6.35$	Periodic
RCA2	25.4	$z = -6.35, 6.35$	Periodic
RCA11	152.4	$z = -69.85, -57.15, -44.45, -31.75, -19.05, -6.35, 6.35, 19.05, 31.75, 44.45, 57.15$	Adiabatic non-slip wall

Non symmetric behavior in the transverse direction observed on temperature, with a lower temperature close to the central injector.

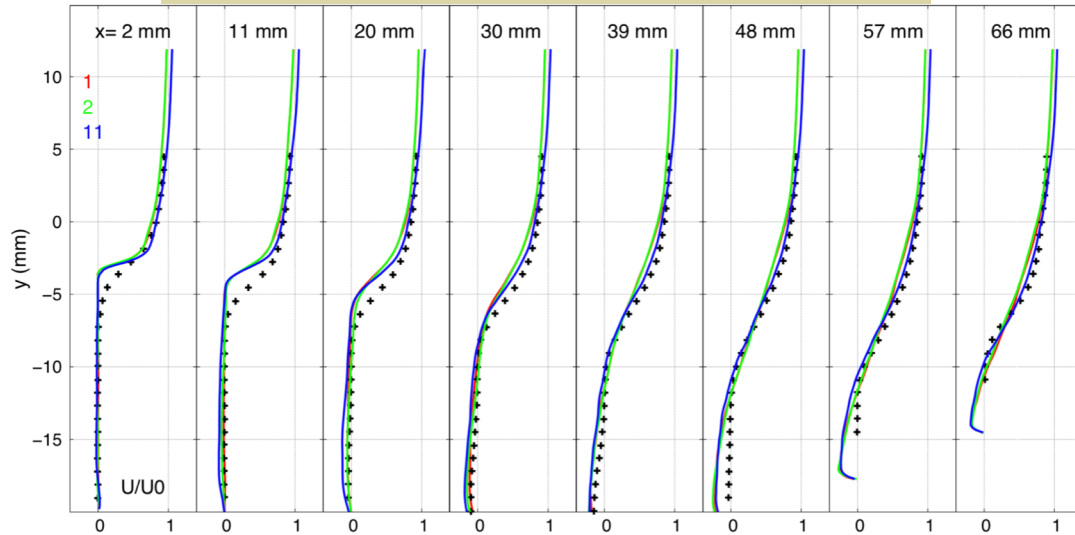
The amount of cold airflow entering through the rear of the cavity is higher in the central injector region, decreasing thus the temperature and the mixture fraction.



Instantaneous isosurface of temperature at 2000 K colored by the values of mixture fraction

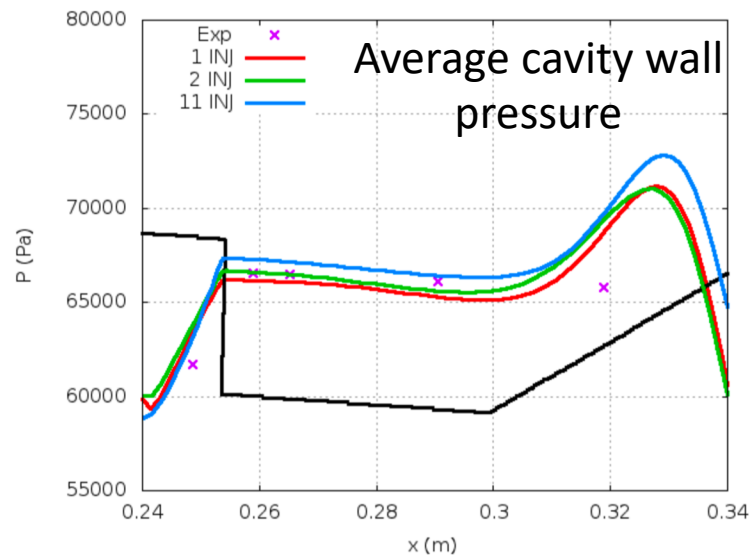
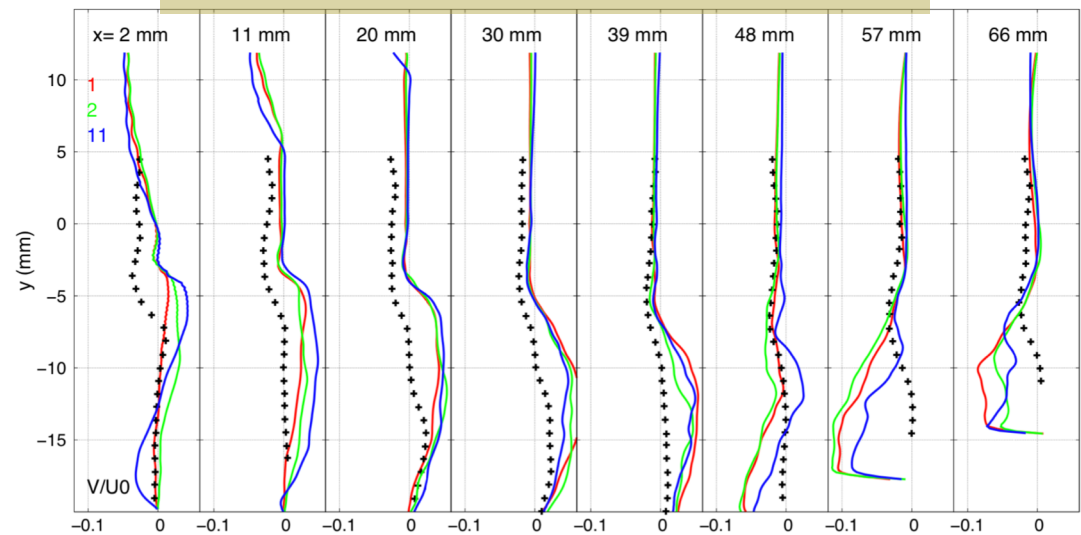
Impact of the number of injectors

Averaged streamwise velocity



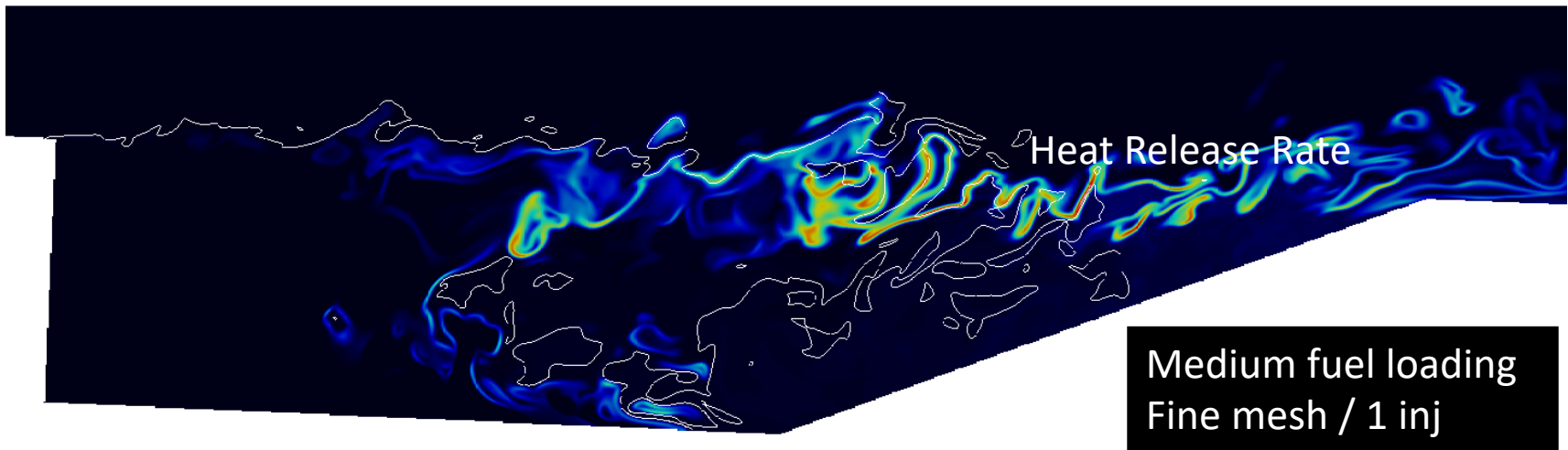
Very few impact on the averaged cavity wall pressure and streamwise velocity (taken between 6th and 7th injector for the case 11 inj.)
Some differences for transverse velocity especially at the cavity rear.

Averaged transverse velocity

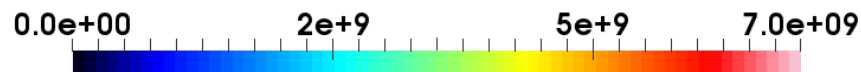


COMBUSTION IN SUPERSONIC FLOWS: the scramjet

- LES using 22 species ethylene reduced scheme in good agreement with available measurements;
- Combustion mainly occurs at low Mach numbers;
- Intricate combustion regimes in the cavity which depend on the ethylene mass flow rate;
- Simplify the geometry to spare cpu time can be misleading;
- *Next step: scramjet with liquid fuel injection, work in progress ...*



Heat Release



COMBUSTION IN SUPERSONIC FLOWS: Flame/Shock Interaction

Hydrogen is a key ingredient to the energy transition:

- Supposing it is produced in an eco-friendly process,
- No green house gases emissions during combustion,
- Can be used to produce electricity (fuel cell),
- Can store surplus of renewable energy from solar or wind farms.

Green Hydrogen



Even produced with an eco-friendly process:

- Highly flammable,
- High susceptibility to leaks resulting in explosion.



Cons



Courtesy of Gangwon Fire HeadQuarter

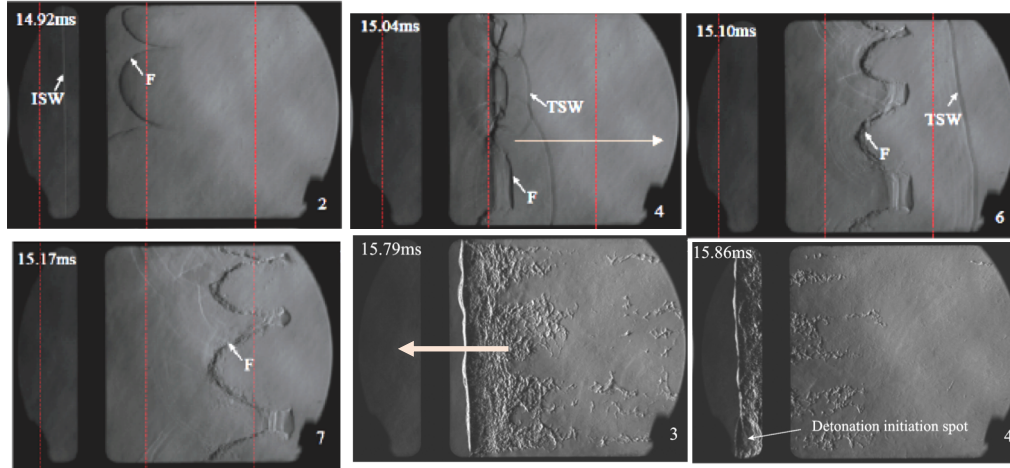
Hydrogen station, South Korea, 2019

The prediction of such a scenario by numerical simulation is therefore necessary in the prevention of disasters.

Oran E. (2015) Understanding explosions - From catastrophic accidents to creation of the universe. Proc. Combust. Inst. 35(1): 1–35.

COMBUSTION IN SUPERSONIC FLOWS: Flame/Shock Interaction

Shock tube = textbook cases to study FSI and DDT.



FSI, $P=17\text{kPa}$, $Ms = 1.9$, $\phi = 1$, Rectangular Tube : 20cm high
M.I. Radulescu H. Yang. 27th ICERS, 2019.

Experiment

« When a weak shock interacts with a flame in a channel, an extremely efficient mechanism for DDT occurs »

FSI : Flame-Shock Interaction

DDT : Deflagration to Detonation Transition

Objective: Understand the early stages of FSI in a H₂/Air mixture and define a reliable numerical set-up

Tool: Direct Numerical Simulation

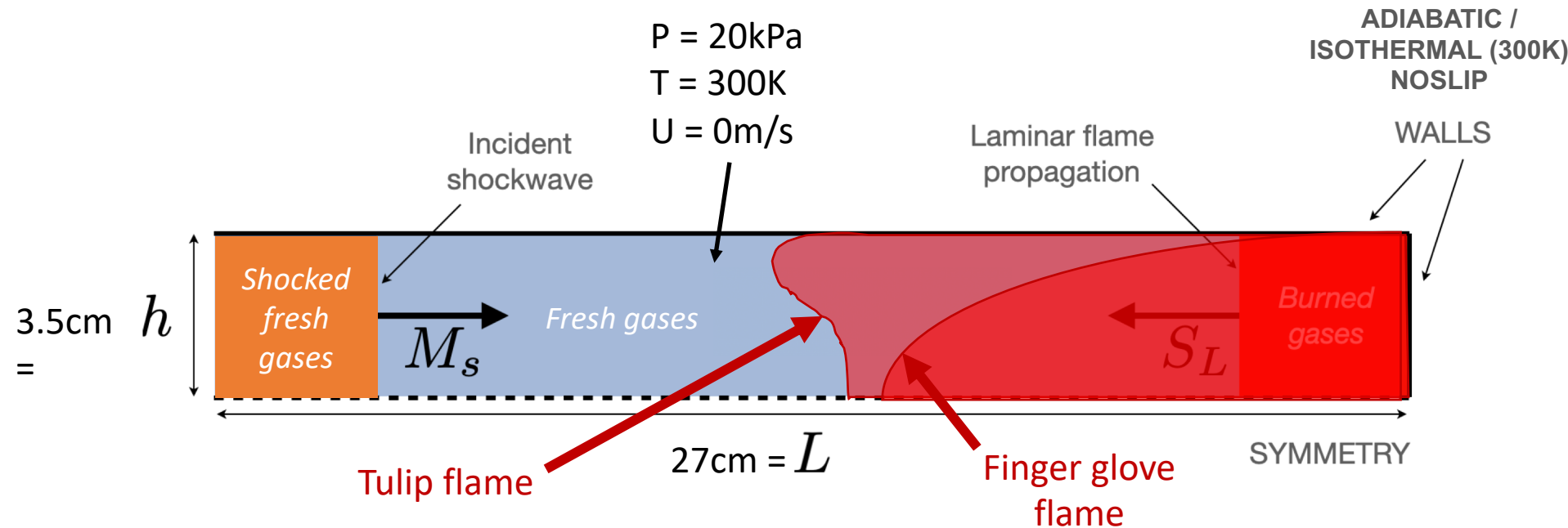
Configuration : Shock-tube under study at ICARE, France (N.Chaumeix's team)

Configuration and numerical set-up

Mach	1.4	1.9
Pressure (kPa)	42.4	80
Temperature (K)	376	483
Velocity (m/s)	227	455

Mixture	H2 - Air
Mechanism	San Diego 9 species, 23 reactions [1]
Equivalence ratio ϕ	0.8
S_L (m/s)	1.77

[1] <https://web.eng.ucsd.edu/mae/groups/combustion/mechanism.html>



➡ 2D Parametric study (16 simulations):

- Two values of the Mach number (1.4 and 1.9) for the incident shock,
- Two initial shapes of the flame (tulip or glove finger) interacting with the incident shock,
- Unity Lewis number for all species versus complex transport properties,
- Cool wall at 300 K versus adiabatic wall condition.

1D Mesh validation for the initial flame

Fresh gases

S_L

Burned gases

REGATH : REal GAs Thermodynamics :
Software (like Chemkin) which calculates 1D
premixed flames[5]

Irregular Mesh : min 10 μm

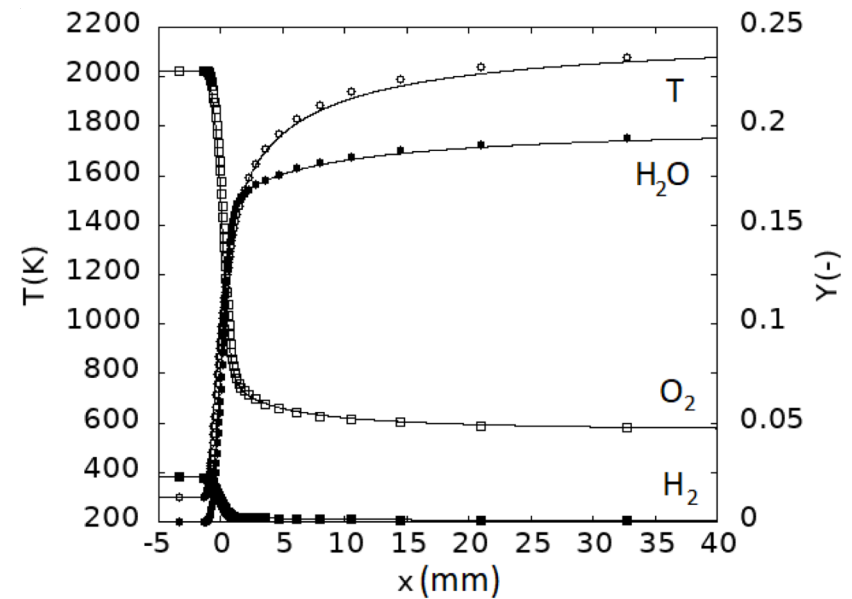
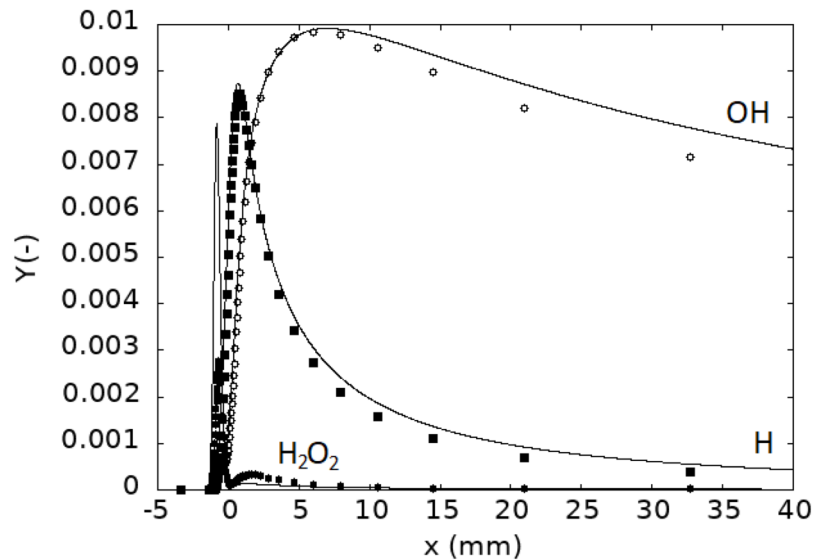
SITCOMB

Regular Mesh : 62.5 μm



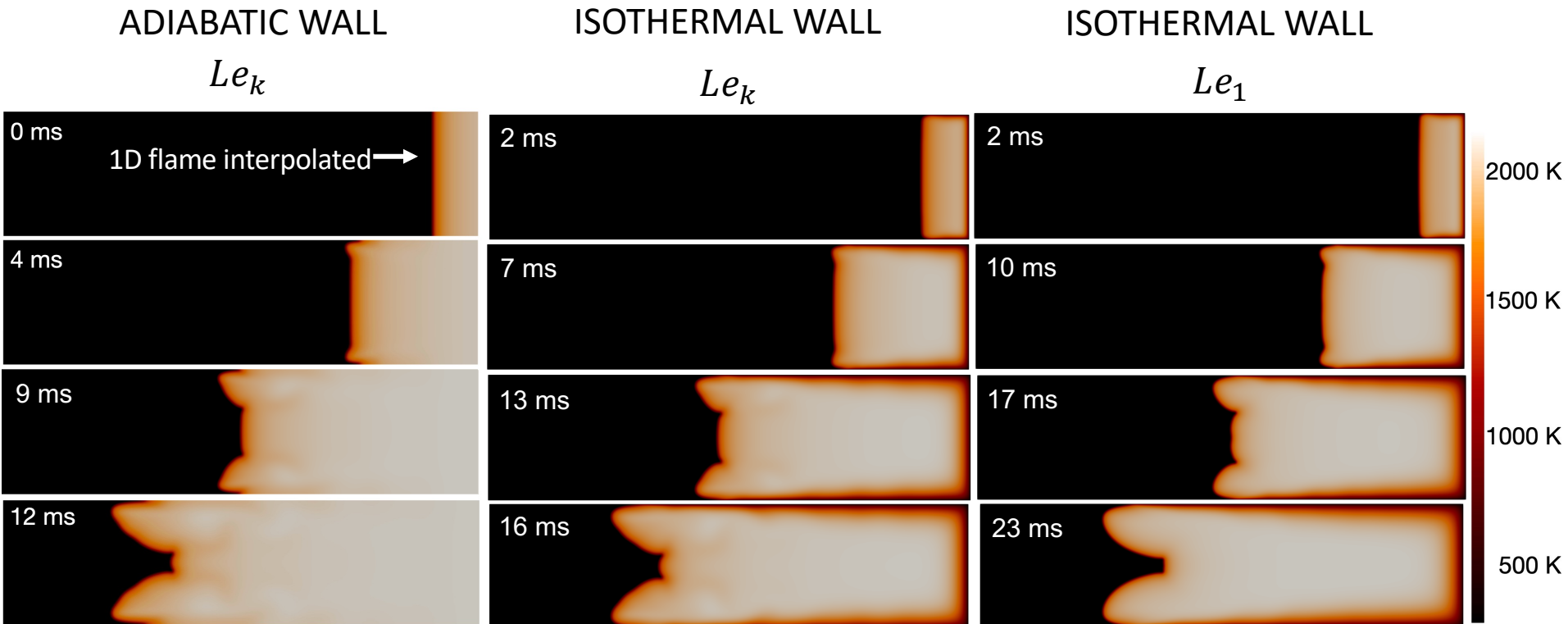
REGATH : lines
SitCom-B : Symbols

$T = 300\text{K}$
 $P = 20\text{kPa}$
 $\phi = 0.8$



2D flame propagation in the semi-closed channel

Initial planar flame as obtained with an ignition with tungsten wires.



Le_k : Complex transport properties

The heat losses on the cold wall slow significantly the flame propagation in the channel.

Unity Lewis assumption leads to a smoother flame surface.

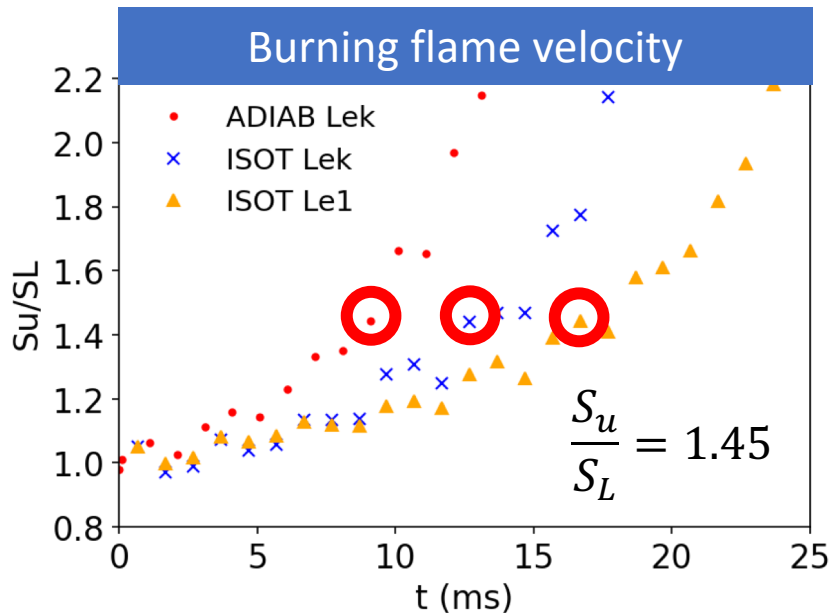
A tulip shape flame is obtained for all three cases.

2D flame propagation in the semi-closed channel

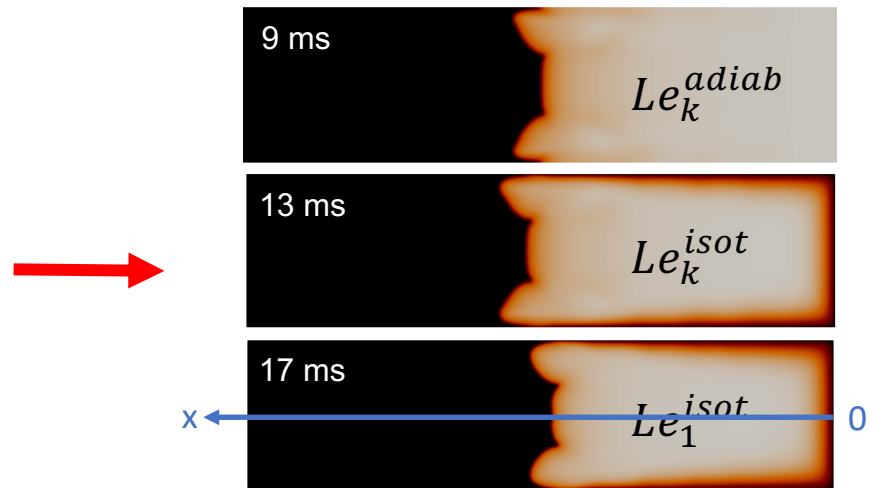
Select an instant for each of the three cases at which the flames will have similar properties.

Burning flame velocity based on H₂O:

$$S_u = \frac{\iint_S \dot{\omega}_{H_2O} dS}{(Y_{H_2O}^b - Y_{H_2O}^u) \rho_u h}$$



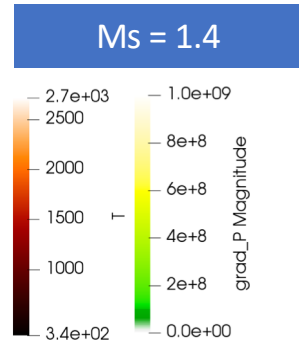
Strong influence of WALLS conditions and transport properties



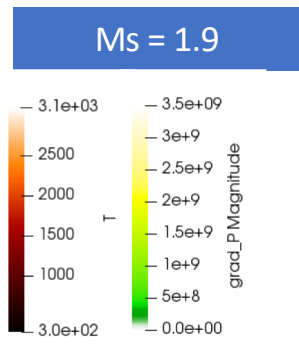
Flame front position on symmetry axis
 $\Delta x < 5\%$

Let's add the incident shock wave

Incident shock Mach impact / adiabatic wall & complex transport properties



$$T_{\max} = 2700K$$



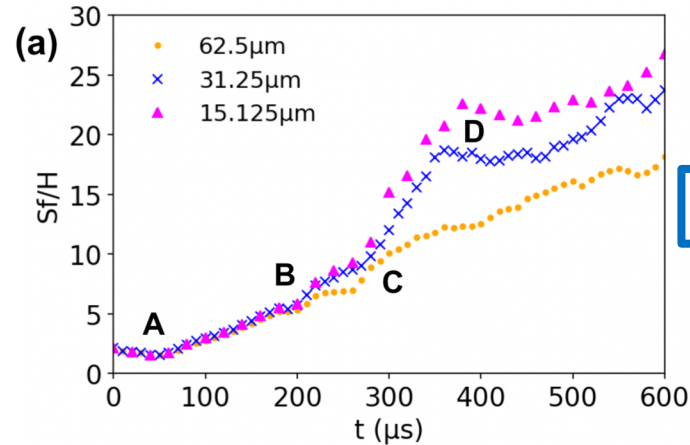
$$T_{\max} = 3100K$$

White line : progress variable, $c = 0.5$

Impact of the mesh resolution with shock addition

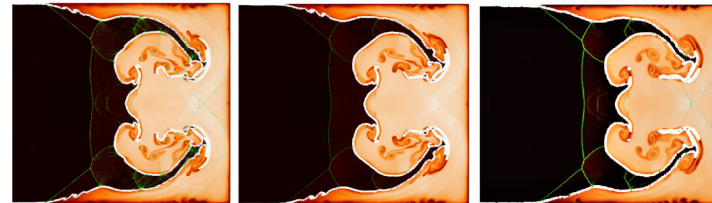
Three resolutions tested:
62.5 μm , 31.25 μm , 15.125 μm

- A:** First encounter of the flame with the incident shock
- B:** Interaction of the flame with the reflected shock
- C:** Apparition of the reactive boundary layer
- D:** Developed reactive BL.



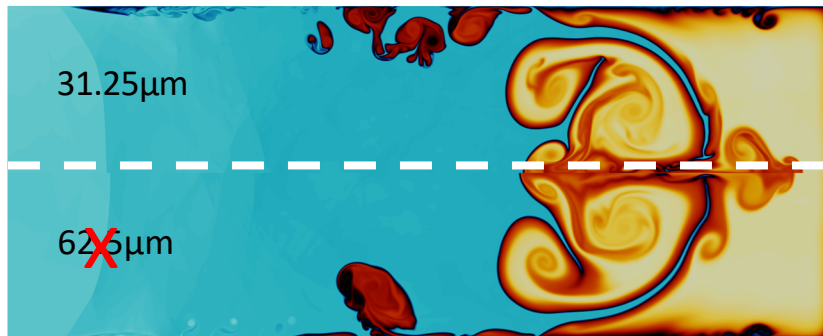
Flame surface

$$S_f = \int_V |\nabla \tilde{c}| dV [7]$$

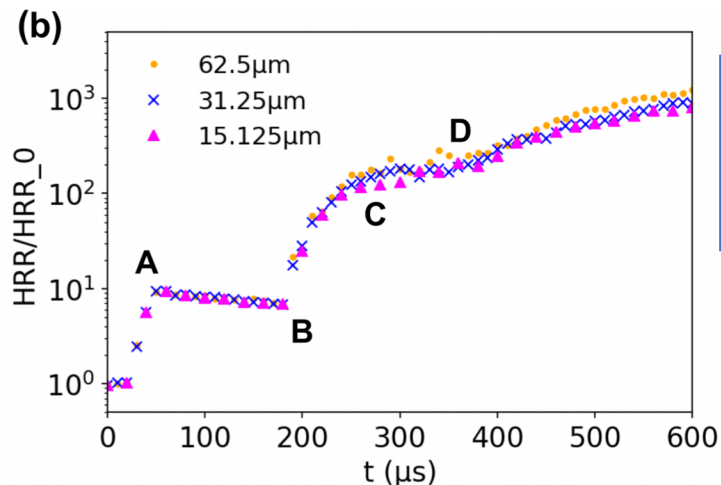


$Ms = 1,9$
 $t = 240\mu\text{s}$

$\Delta x_i = 15.125 \mu\text{m}$ $\Delta x_i = 31.25 \mu\text{m}$ $\Delta x_i = 62.5 \mu\text{m}$



$Ms = 1.4, t = 560\mu\text{s}$



Heat release
conditioned
at $c=0.5$

Adiabatic versus isothermal walls (complex transport)

$M_s=1.4$

ADIABATIC

ISOTHERMAL

160 μ s

120 μ s

Curved shock

260 μ s

240 μ s

Instabilities more developed

320 μ s

300 μ s

Efficient reactive boundary layer

Reduced reactive boundary layer

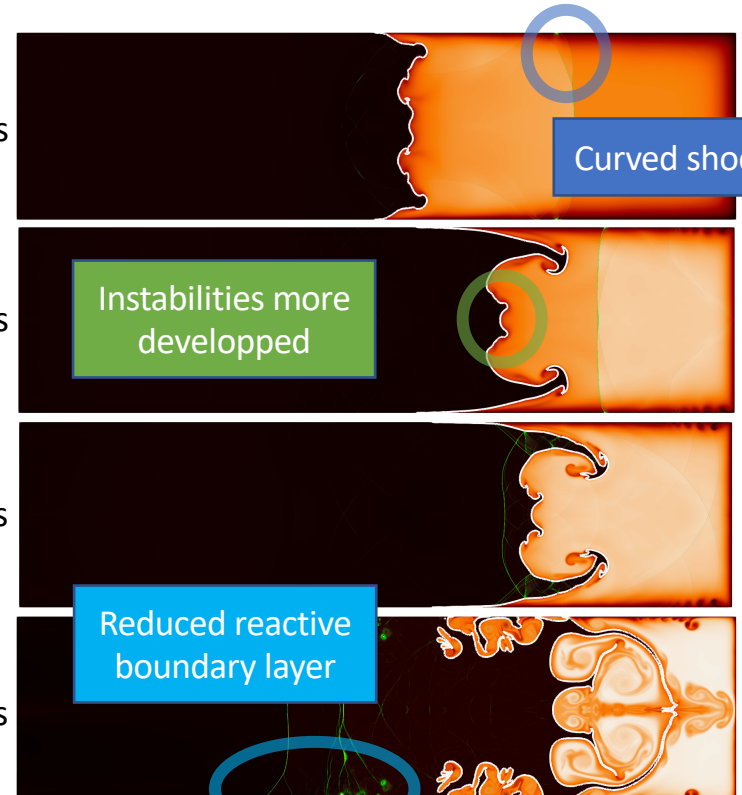
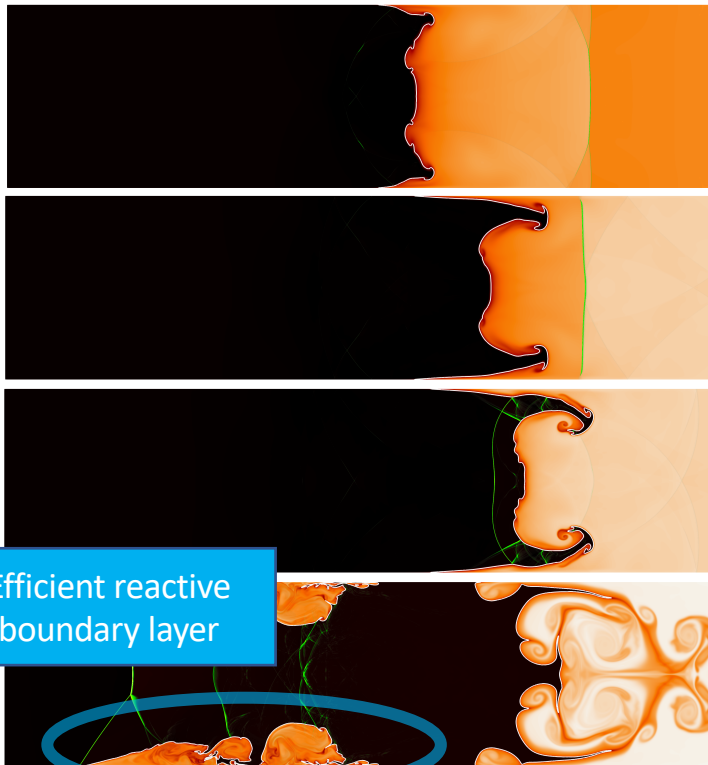
760 μ s

620 μ s

Richtmyer-Meshkov instabilities

Kelvin-Helmoltz instabilities

Boundary layer =
opportunity for the combustion to develop

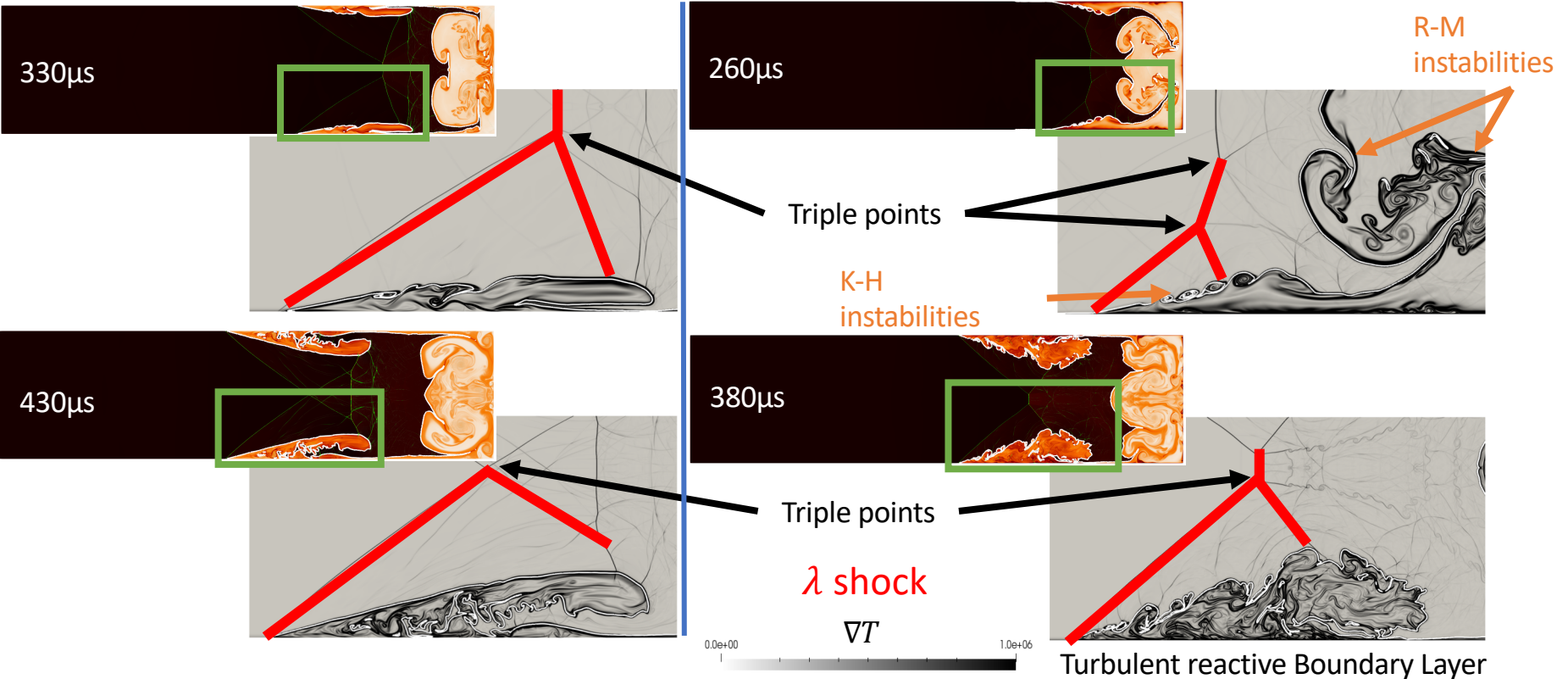


Adiabatic versus isothermal walls (complex transport)

$Ms=1.9$

ADIABATIC

ISOTHERMAL



Adiabatic versus isothermal walls (complex transport)

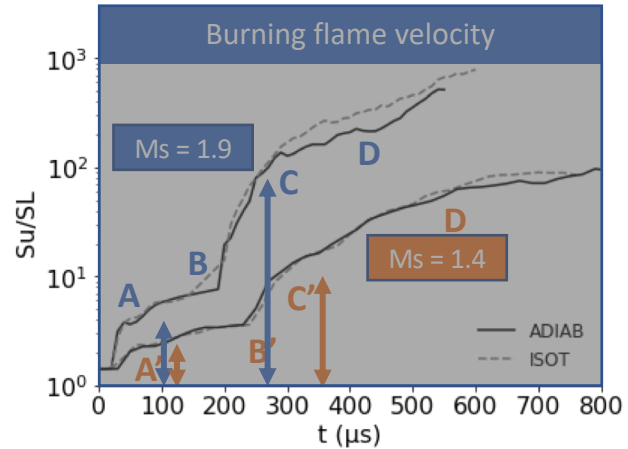
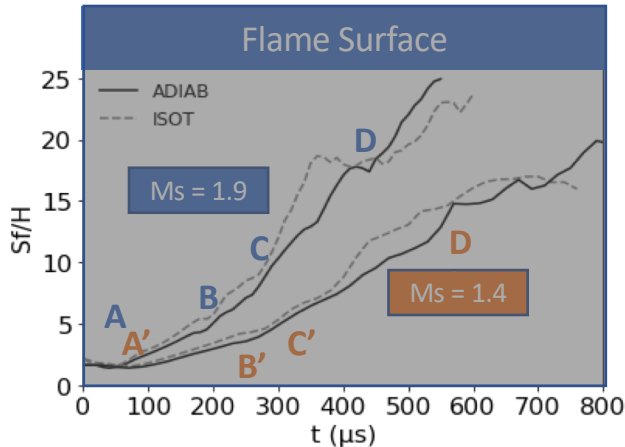
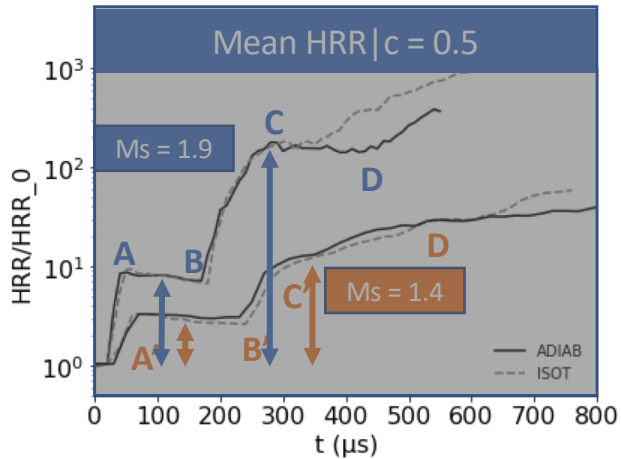
$$\langle \text{HRR} | c=0.5 \rangle$$

$$\text{HRR}_0 = 2.5e8 \text{ W/m}^3$$

$$\langle \text{HRR} | c=0.5 \rangle \text{ 1D flame}$$

$$S_f = \int_V |\nabla \tilde{c}| dV \quad [7]$$

$$S_u = \frac{\iint_S \dot{\omega}_{\text{H}_2\text{O}} dS}{(Y_{\text{H}_2\text{O}}^b - Y_{\text{H}_2\text{O}}^u) \rho_u h}$$



A : HRR x 10
C : HRR x 200

A' : HRR x 3
C' : HRR x 10

$S_{f\text{ISOTHERMAL}} > S_{f\text{ADIABATIC}}$
until BL well developed

($H = 7\text{cm}$)

A : S_u/SL x 4
C : S_u/SL x 100

A' : S_u/SL x 2
C' : S_u/SL x 10

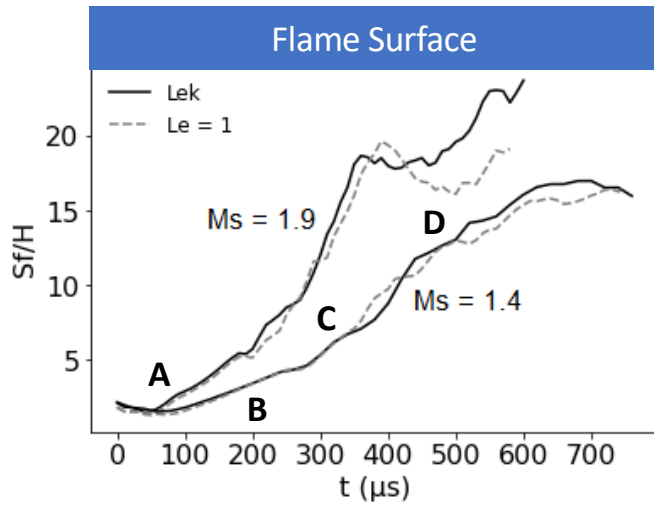
A : 1st FSI
B : 2nd FSI
C : Beginning of Boundary Layer (BL)
D : BL hooked on lambda shock

FSI : Flame-Shock Interaction

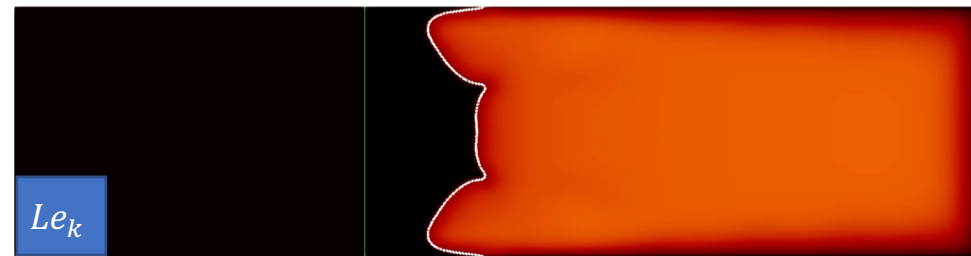
Moderate impact of wall conditions on global variables
Incident shock Mach number = key control parameter

Complex transport properties versus unity Lewis number

Characteristic times : $\tau_{FSI} \approx 0.03 \text{ ms} < \tau_f = \frac{\delta_f}{S_L} \approx 0.2 \text{ ms}$



$Ms = 1.4$
 $T_{\text{wall}} = 300 \text{ K}$



Impact of the diffusion of the species could be neglected during FSI.

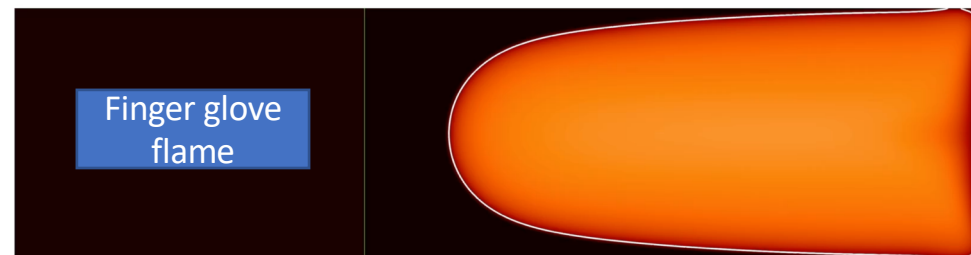
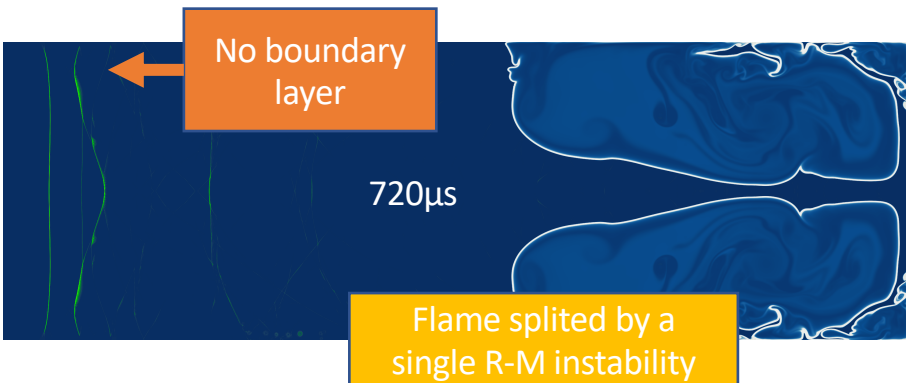
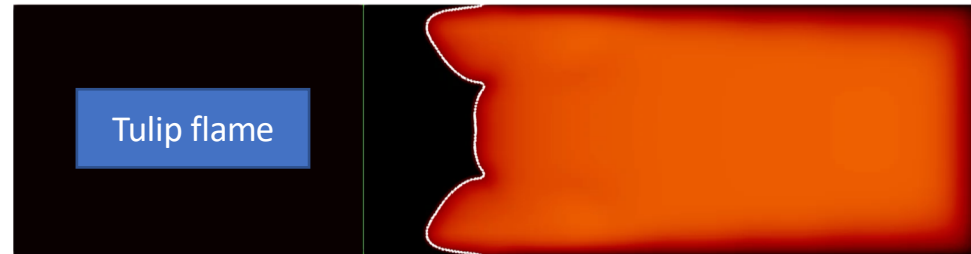
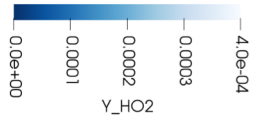
A : 1st FSI
B : 2nd FSI
C : Beginning of Boundary Layer (BL)
D : BL hooked on lambda shock

FSI : Flame-Shock Interaction

Unity Lewis assumption hampers the development of the reactive boundary layer compared to complex transport.

Influence of the shape of the flame before FSI

$Ms = 1.4$, $T_{wall} = 300$, Complex transport



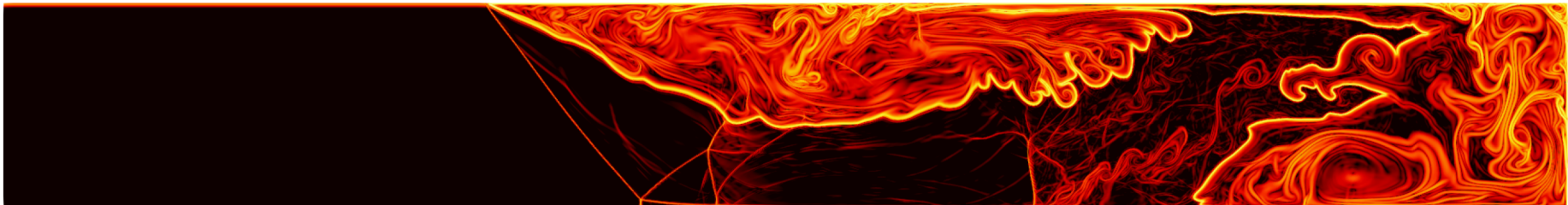
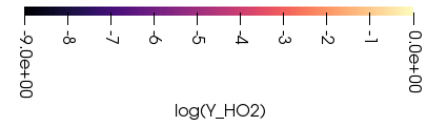
However, whatever the flame shape, global variables (burning velocity, flame surface, heat release) converge to a same order of magnitude for a given Mach number !

Conclusion

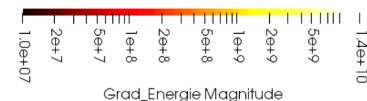
- The incident shock Mach number is the key parameter for both FSI and BL characteristics;
- Wall thermal conditions and modeling of transport properties have a moderate impact on the FSI;
- Wall thermal conditions and modeling of transport properties have a significant impact on reactive BL development;
- Next steps: comparison with experimental results (collaboration with N. Chaumeix from ICARE) / develop analyzing tools



Ms=1.4, ISOTHERMAL WALLS, Complex Transport / HO₂ concentration



Ms=1.9, ISOTHERMAL WALLS, Complex Transport / gradient of total energy



Thank you for your attention!

The place to be in April 2023



APRIL 26-28, 2023
ROUEN, FRANCE

Thanks to GENCI and CRIANN for CPU time.

Thanks to ANR, DGA and Regional council of Normandy for funding.



RÉGION
NORMANDIE



Agence Nationale de la Recherche

DGA ANR

